Transient Model for CW and Pulsed Laser Machining of Ablating/Decomposing Materials— Approximate Analysis

Michael F. Modest, Fellow ASME
Professor of Mechanical Engineering
The Pennsylvania State University
University Park, PA 16802

Abstract

Approximate, quasi-onedimensional conduction models have been developed to predict the changing shape of holes, single grooves, or overlapping grooves carved by ablation into a thick solid that is irradiated by a moving laser source. For CW or pulsed laser operation a simple integral method is presented, which predicts shapes and removal rates with an accuracy of a few percent, while requiring one order of magnitude less CPU time than a three-dimensional, numerical solution. For pulsed operation a “full pulse” model is presented, computing the erosion from an entire pulse in a single step, and reducing computer time by another order of magnitude.

Nomenclature

a	curvature parameter, eq. (15)
c	specific heat
C_1, C_2, C_3	constants in Arrhenius relation
dA	infinitesimal cross sectional area
F	irradiation flux vector
F_0	radiation flux density at center of beam at focal plane
Δh_{re}	"heat of removal"
î,ĵ,k̂	unit vector in x, y and z directions
k	thermal conductivity
n̂	unit surface normal
N_k	conduction-to-laser power parameter
Q	dimensionless irradiation flux vector at surface, = $\mathbf{F}/F_0$
$\bar{s}(\bar{x}, \bar{y})$	local groove depth
$s(x, y)$	dimensionless groove depth
Ste	Stefan number (ablation energy-to-sensible heat parameter)
$\bar{t}$	time
t	dimensionless time
T	temperature
u	laser scanning speed
U	laser speed-to-diffusion speed parameter
v_n	ablation velocity (of solid surface)
w, w_0	$1/e^2$ radius of laser beam (at focal plane)
W	dimensionless radius of laser beam, = w/w_0
$\bar{x}, \bar{y}, \bar{z}$	Cartesian coordinates
x, y, z	dimensionless Cartesian coordinates
Greek Letters	
α_H	thermal diffusivity
α	local effective absorptivity at laser wavelength
β_∞	far-field beam divergence
δ	temperature penetration depth
λ	wavelength of laser radiation
ρ	density of the medium
θ, θ_0	dimensionless temperature (at the surface)
Subscripts	
re	evaluated at evaporation (or decomposition) temperature
∞	evaluated at ambient conditions, or located far away

Introduction

Since their invention in 1960, lasers have found diverse applications in engineering and industry because of their ability to produce high-power beams. Laser applications include welding, drilling,

cutting, scribing, machining, heat treatment, medical surgery, and others. One of the principle advantages of laser cutting is its ability to cut very hard materials easily. Ceramics are among the most difficult materials to machine by conventional machining techniques, since they are very hard and brittle. The cost of machining ceramics into complex shapes is often prohibitive if conventional machining is used. Lasers may provide a cheaper alternative to conventional machining and have found wide-spread use in industry.

Modeling of laser drilling, cutting and scribing has been addressed by a number of investigators. Simple one-dimensional drilling models have been given by Dabby and Paek (1972) and Wagner (1974). Other approximate laser drilling models have been developed by von Allmen (1976), Petring *et al.* (1988), and others. Multiple reflections during laser drilling have been addressed by Anthony (1980), Bailey and Modak (1989), Vorreiter *et al.* (1991) and Ramanathan and Modest (1992b).

Simple cutting models have been developed by Bunting and Cornfield (1975), and by the group around Schuöcker, e.g., Schuöcker and Müller (1987), and Modest and Ramanathan (1992a).

Laser scribing of ablating and/or decomposing materials has been investigated primarily by Modest and coworkers. They developed a number of simple models for quasi-steady CW laser scribing, e.g., Modest and Abakians (1986) and Ramanathan and Modest (1990), as well as sophisticated 3-D models for CW as well as pulsed lasers, e.g., Roy and Modest (1993), Bang *et al.* (1993), Modest (1995) and Modest *et al.* (1994).

Finally, simple modeling of 3-D machining with a dual beam has been presented by Chryssoloris (1991).

While sophisticated 3-D models describing the grooving process, such as Modest (1995), are able to accurately predict groove shapes, this accuracy is only as good as the knowledge of relevant material properties (which is generally poor). In addition, these models tend to demand vast amounts of computer time, due to their nonlinearity as well as their three-dimensionality. Therefore, it would be highly desirable to have a simple, approximate model that can predict transient and pulsed shaping processes, similar to the approximate model of Modest and Abakians (1986) for quasi-steady CW laser grooving. In the following, two such approximate models are developed. Comparison with "exact" three-dimensional calculations will show that these models can reduce computer times by orders of magnitude, accompanied by only a minor loss in accuracy.

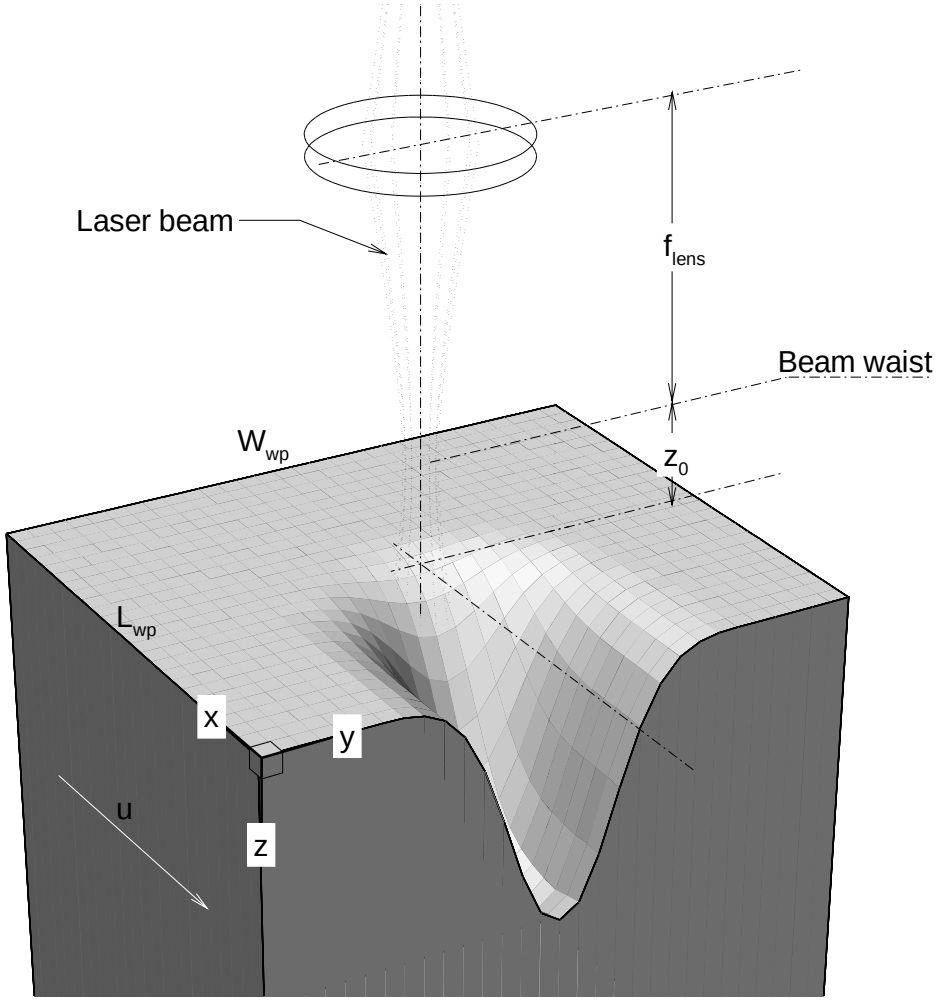

Figure 1: Laser machining setup and coordinate system.

Theoretical Background

A sketch for the problem under consideration is given in Fig. 1. Simplifying assumptions for the present model are identical to the assumptions for the fully three-dimensional model of Modest (1995); for convenience and to clarify the applicability and limitations of the model, they are repeated here:

1. The solid moves with constant velocity u.
2. The solid is isotropic.
3. Property variations of the solid with temperature are negligible. Numerical experiments with two- and three-dimensional models have shown that, even for ceramics with thermal

diffusivity variations close to a full order of magnitude, this assumption is adequate provided properties are evaluated at the ablation temperature [Ramanathan and Modest (1990), Roy and Modest (1993)].

4. The material is opaque, i.e., the laser beam does not penetrate appreciably into the medium. This assumption is somewhat limiting since some ceramics and other nonmetals are relatively transparent at shorter wavelengths (i.e., at YAG and excimer laser wavelengths). Even the opaquest material becomes semitransparent during ultra-short pulses compared to thermal penetration by conduction, which may only be a fraction of a μm. Fortunately, for such cases conductive losses are negligible.
5. Change of phase from solid to vapor (or decomposition products) occurs in a single step with a rate governed by a simple Arrhenius relation. This assumption is relatively good for a number of ceramics and other nonmetals, in particular since the exact removal process is not well understood for many materials to date. For example, graphite is expected to ablate, silicon carbide to decompose into various gases, and silicon nitride to decompose into nitrogen and liquid silicon [forming a very thin liquid layer; with droplets being expelled, Ramanathan and Modest (1995)]. Alumina is known to melt, but the liquid layer may be thin enough due to alumina's low thermal diffusivity. On the other hand the present model is unsuitable for metals, which are expected to form thick liquid layers, possibly with strong convection.
6. The evaporated material does not interfere with the incoming laser beam and ionization of the gas does not occur. Most laser machining devices are outfitted with strong gas assists, which have the purpose of (i) protecting the lens, (ii) blowing debris out of the way, and (iii) suppressing or aiding chemical reactions on the material's surface. Thus, for nonmetals, this assumption is generally good. For metals plasma formation is commonly observed and beam interaction with free electrons is likely in spite of strong gas assist.
7. Heat losses by convection and radiation are negligible as compared to the intensity of the incident beam. Such losses could easily be included in the analysis. However, Modest and Abakians (1986) have shown these effects to be negligible for virtually all situations, including a sonic assist jet blowing across the surface.
8. Multiple reflections of laser radiation within the groove are neglected. This limits the present analysis to strongly absorbing media and/or shallow grooves. Multiple reflections effects

have been studied by Bang and Modest (1991,1992) and Bang et al. (1993). Their reflection models could be combined with the present analysis.

As a consequence of these assumptions it is clear that the present analysis is aimed at non-melting ceramics and other nonmetals. For the present theory we will also assume, in addition to the above, that conduction losses are relatively minor, i.e., if conduction losses are less than, say, 25% of total absorbed laser energy and if these losses can be predicted with, say, 20% acuracy, the overall error would be below $0.25 \times 0.20 = 5\%$.

Following Modest (1995) the transient heat conduction equation for a thick solid irradiated by a scanning Gaussian laser beam, and its auxiliary conditions, may be written in non-dimensional form as

$$\frac{\partial \theta}{\partial t} = \nabla^2 \theta, \tag{1}$$

Initial condition:

$$t = 0: \quad \theta(x, y, z, 0) = 0 \tag{2}$$
$$s(x, y, 0) = s_0(x, y),$$

Boundary conditions:

$$x \to \pm\infty, \qquad y \to \pm\infty, \qquad z \to +\infty: \qquad \theta = 0; \tag{3}$$
$$z = s(x, y, t): \qquad \alpha \mathbf{Q} \cdot \hat{\mathbf{n}} = -N_k [\hat{\mathbf{n}} \cdot \nabla \theta - V_n \mathrm{Ste}];$$

Ablation condition:

$$z = s(x, y, t): \qquad V_n = C_1 e^{C_2[1 - T\mathrm{re}/T(\theta)]}, \tag{4}$$

with

$$x = \bar{x}/w_0; \quad y = \bar{y}/w_0; \quad z = \bar{z}/w_0; \quad s = \bar{s}/w_0; \quad \tau = \alpha_H \bar{t}/w_0^2; \quad \theta = \frac{T - T_\infty}{T_{\mathrm{re}} - T_\infty}; \tag{5}$$
$$U = \frac{u w_0}{\alpha_H}; \quad V_n = \frac{v_n w_0}{\alpha_H}; \quad N_k = \frac{k(T_{\mathrm{re}} - T_\infty)}{F_0 w_0}; \quad \mathrm{Ste} = \frac{\Delta h_{\mathrm{re}}}{c(T_{\mathrm{re}} - T_\infty)}.$$

Here $\bar{x}, \bar{y}, \bar{z}$ and $\bar{s}$ are dimensional coordinates and groove depth, which are then nondimensionalized with the beam radius at the focal point, w_0; $\alpha_H = k/\rho c$ is the thermal diffusivity of the material, T_{re} is the equilibrium ablation (or "removal" temperature), and Δh_{re} is the energy required to

remove material ("heat of removal"). The parameters U and V_n are nondimensional laser scanning and (transient) surface recession velocities (by ablation), N_k approximates the ratio of conduction losses, for a surface normal to irradiation, and the absorbed laser flux; and Ste is the Stefan number that compares ablation energy with sensible heat.

The boundary condition at the top surface, $z = s(x, y, t)$, specifies that absorbed laser irradiation is used up by conduction losses and by the latent heat required to ablate material. The ablation velocity (normal to the surface) is governed by a simple reaction equation of the Arhennius type [Modest (1995)].

The energy intensity distribution, **F**, for a focussed Gaussian laser beam having a waist w_0 at the focal plane z_0 and a total average power of $P = \frac{\pi}{2} F_0 w_0^2$ is given by Kogelnik and Li (1956), and for a laser moving with constant velocity u into the positive $\bar{x}$ direction is:

$$\mathbf{Q} = \frac{\mathbf{F}}{F_0} = \frac{\phi(t)}{W^2} \exp\left[-2\frac{(x - Ut)^2 + y^2}{W^2}\right] \frac{\hat{\mathbf{s}}}{\hat{\mathbf{s}} \cdot \hat{\mathbf{k}}}, \tag{6}$$

where

$$W^2(z) = \frac{w^2(z)}{w_0^2} = 1 + \beta_\infty^2 (z - z_0), \tag{7}$$

defines the beam radius, w, away from focus and

$$\beta_\infty = \frac{\lambda}{\pi w_0} \tag{8}$$

is the far-field beam divergence angle for the diffraction-limited case of a Gaussian beam. If the laser beam is visualized as consisting of a bundle of rays into the direction $\hat{\mathbf{s}}(x, y, z)$, perpendicular to the wave-front of propagation, then $\hat{\mathbf{s}}$ can be related to the radius of the wave-front [Luxon and Parker (1985)], $r_c(z)$, as:

$$\frac{\hat{\mathbf{s}}}{\hat{\mathbf{s}} \cdot \hat{\mathbf{k}}} = \frac{(x - Ut)\hat{\mathbf{i}} + y\hat{\mathbf{j}}}{\sqrt{r_c^2(z) - x^2 - y^2}} + \hat{\mathbf{k}}, \tag{9}$$

$$r_c(z) = (z - z_0)\left[1 + \frac{1}{\beta_\infty^2 (z - z_0)^2}\right]. \tag{10}$$

Results given in this paper are limited to the Gaussian laser described above to simplify their presentation; arbitrary spatial intensity profiles are readily incorporated.

Finally, $\phi(t)$ defines the temporal intensity variation during a laser pulse period of duration $t_p = t_{p,\text{on}} + t_{p,\text{off}}$, and is normalized such that

$$\frac{1}{t_p}\int_t^{t+t_p} \phi(t)dt = 1. \tag{11}$$

Therefore, for a CW laser $\phi \equiv 1$.

Solution Approach

Equation (1) with its auxiliary conditions (2) through (4) form a complete set of dimensionless equations in transient form to predict the forming groove shape $s(x, y, t)$ and temperature field $\theta(x, y, z, t)$. In order to find a simple, approximate solution for the conduction loss, equation (1), we will assume that conduction takes place only in the direction of the (local) surface normal, i.e., the loss is locally one-dimensional. Transforming coordinates to n, a nondimensional distance from a surface location pointing into the medium along the local surface normal (see Figure 2), the solid will move through the origin for n with the ablation velocity V_n into the negative n-direction. Thus, equation (1) transforms to

$$\frac{\partial}{\partial t}(dA\,\theta) - V_n\frac{\partial}{\partial n}(dA\,\theta) = \frac{\partial}{\partial n}\left(dA\frac{\partial\theta}{\partial n}\right), \tag{12}$$

where $dA(n)$ is a local conduction cross section (Fig. 2). Inclusion of the factor $dA(n)$ allows to estimate surface curvature effects, which enhance conduction losses (concave surface, as shown in Fig. 2) or impede them (convex surface, e.g., near the rim of the groove). If

$$\mathbf{r}(x, y, n) = \mathbf{r}(x, y, 0) + n\hat{\mathbf{n}} = x\hat{\mathbf{i}} + y\hat{\mathbf{j}} + s\hat{\mathbf{k}} + n\hat{\mathbf{n}} \tag{13}$$

is the vector to a point along n, then the cross-sectional area may be calculated from

$$dA(n) = \left|\frac{\partial\mathbf{r}}{\partial x}\right|\left|\frac{\partial\mathbf{r}}{\partial y}\right| dx\; dy. \tag{14}$$

Evaluating equation (14) up to $\mathcal{O}(n)$ (since the heat-affected zone is expected to be thin), one finds

$$dA(n) = dA(0)\left[1 + an + \mathcal{O}(n^2)\right], \tag{15}$$

$$a = -\frac{1}{\sqrt{1 + s_x^2 + s_y^2}}\left[\frac{s_{xx}}{1 + s_x^2} + \frac{s_{yy}}{1 + s_y^2}\right],$$

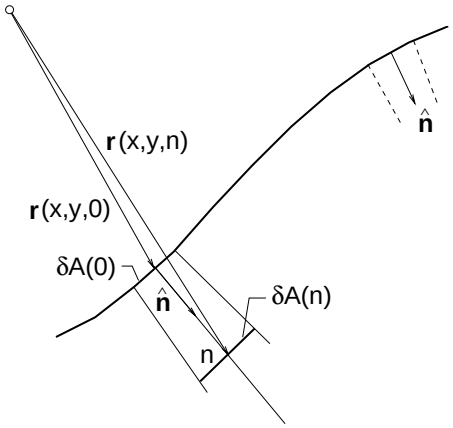

Figure 2: Local coordinate system into direction of surface normal.

where the subscripts denote differentiation, i.e., $s_x = \partial s/\partial x$, etc. Equation (12) is readily solved approximately using an integral method with a chosen temperature profile

$$\theta \simeq \theta_0 e^{-n/\delta}, \tag{16}$$

where θ_0 is local surface temperature and δ is a measure of the local penetration depth. Using this profile to satisfy equation (12) in an integral sense (i.e., integrating the equation over all n from 0 to ∞), and again using equation (16) in boundary condition (3), leads to three simultaneous, nonlinear equations for the unknown values of θ_0, V_n and δ, which are all functions of surface location and time:

$$\frac{d}{dt}\left[\theta_0\delta(1+a\delta)\right] + V_n\theta_0 = \frac{\theta_0}{\delta}, \tag{17}$$

$$\frac{\theta_0}{\delta} = \frac{\mathbf{Q}\cdot\hat{\mathbf{n}}}{N_k} - V_n\mathrm{Ste}, \tag{18}$$

$$V_n = C_1\exp\left[C_2\frac{\theta_0 - 1}{\theta_0 + C_3}\right], \qquad C_3 = \frac{T_\infty}{T\mathrm{re} - T_\infty}. \tag{19}$$

The last equation is simply the ablation condition, equation (4), which relates surface temperature to the ablation velocity, which in turn is related to the receding groove depth by

$$\frac{ds}{dt} = \frac{V_n}{\hat{\mathbf{n}}\cdot\hat{\mathbf{k}}} \tag{20}$$

Equations (17) through (20) must be solved simultaneously to obtain an expression for the surface topology, $s(x, y, t)$.

It is important to realize that equation (16) is a rather simplistic temperature profile and that the solution to equations (17) through (20) is going to be satisfacotry only as long as the temporal variation of $\mathbf{Q} \cdot \hat{\mathbf{n}}$ allows this profile to be acceptable. In particular, equation (16) cannot have an inflection point and is, therefore, unable to predict the trends after laser power has been turned off abruptly. Fortunately, extensive numerical experiments with the "exact" 3D-code show that ablation ceases almost immediately after the laser is turned off, making a solution of equations (17) through (20) unnecessary for those times.

Pulsed Lasers

Equations (17) through (20) are equally applicable to continuous-wave as well as pulsed lasers. However, for pulsed lasers ablation takes place only during the laser-on periods, and conduction losses are generally very small. Therefore, it should be possible to simplify the governing equations even further, and still arrive at a reasonably-accurate prediction for the forming surface topography. This may be achieved by breaking up each laser pulse into three separate, idealized stages: (1) a heat-up period of duration t_1, during which the underlying material is heated to ablation conditions, but during which no ablation occurs (V_n = 0), (2) ablation of duration $t_{p,\text{on}} - t_1$, during which a fully-established heat-affected zone is pushed into the material along with the ablation front [i.e., the rate of change of heat stored in the substrate–the first term in equation (17)–is negligible as compared with ablation energy, $V_n(\theta_0$+Ste)], and (3) a cool-down period (the laser-off time $t_{p,\text{off}}$), during which the solid cools back to ambient conditions. It is this internally stored preheat energy at the end of the second period that constitutes the conductive loss. Thus, we have:

Heat-up Period:

$$\frac{d}{dt}\left[\theta_0\delta(1 + a\delta)\right] = \frac{\mathbf{Q} \cdot \hat{\mathbf{n}}}{N_k}, \qquad 0 < t < t_1, \tag{21}$$

or

$$\theta_0\delta(1 + a\delta)(t_1) = \int_0^{t_1} \frac{\mathbf{Q} \cdot \hat{\mathbf{n}}}{N_k} dt \tag{22}$$

Ablation Period:

$$V_n\theta_0 = \frac{\theta_0}{\delta} = \frac{\mathbf{Q} \cdot \hat{\mathbf{n}}}{N_k} - V_n\text{Ste}, \qquad t_1 \leq t \leq t_{p,\text{on}}, \tag{23}$$

or

$$V_n(t) = \frac{1}{\delta} = \frac{\mathbf{Q} \cdot \hat{\mathbf{n}}(t)}{N_k(\theta_0 + \text{Ste})}, \tag{24}$$

and the ablation temperature follows from equation (19). It is the nature of an Arrhenius rate equation that ablation temperature remains almost constant ($\theta_0 \simeq$ const = $\bar{\theta}_0 \simeq 1$), even through the ablation rate may vary strongly with $\mathbf{Q} \cdot \hat{\mathbf{n}}(t)$. Thus, equation (24) may be further simplified replacing $\theta_0(t)$ by an average value $\bar{\theta}_0$, which may be determined by inverting equation (19) in terms of an average ablation velocity,

$$\bar{\theta}_0 = \frac{1 + C_3}{1 - \frac{1}{C_2} \ln\left(\frac{\bar{V}_n}{C_1}\right)} - C_3, \tag{25}$$

$$\bar{V}_n = \frac{1}{t_{\text{p,on}} - t_1} \int_{t_1}^{t_{\text{p,on}}} V_n dt = \frac{\int_{t_1}^{t_{\text{p,on}}} \mathbf{Q} \cdot \hat{\mathbf{n}} dt}{(t_{\text{p,on}} - t_1)(\bar{\theta}_0 + \text{Ste})}. \tag{26}$$

The two solutions (heat-up and ablation) may be mated by specifying the heat-up period to have ended when θ_0 reaches the value $\bar{\theta}_0$ and $\delta(t_1)$ is assumed to have reached the value given by equation (24) at $t = t_1$: t_1 is determined from this condition. The solution proceeds as follows:

1) A t_1 is guessed [an accurate first guess is obtained from equation (22) since it is known that $\bar{\theta}_0 \simeq 1$].

2) An average ablation velocity is obtained from equation (26) (again, starting with $\bar{\theta}_0 \simeq 1$).

3) A new value for $\bar{\theta}_0$ is obtained from equation (25).

4) Updated values for $\delta(t_1)$ and t_1 are found from equations (24) and (22), respectively.

Converged values for $\bar{\theta}_0$ and t_1 are then found through iteration. The situation is particularly simple for a basic on-off pulse [$\phi(t) = t_p/t_{p,\text{on}}$ = const for $t < t_{p,\text{on}}$, $\phi(t) = 0$ otherwise]. In that case $\mathbf{Q} \cdot \hat{\mathbf{n}}$ = const during laser-on time, and ablation proceeds quasi-steady with V_n, δ, θ_0 all being constant. Then, for an on-off pulse,

$$\bar{V}_n = V_n = \frac{1}{\delta} = \frac{\mathbf{Q} \cdot \hat{\mathbf{n}}}{N_k(\theta_0 + \text{Ste})} = \text{const}, \tag{27}$$

$$t_1 = \frac{N_k}{\mathbf{Q} \cdot \hat{\mathbf{n}}} \theta_0 \delta (1 + a\delta). \tag{28}$$

For any temporal pulse shape, the updated local groove depth after the ith pulse, s_i, follows then from equation (20) as

$$s_i(x, y) = s_{i-1}(x, y) + \frac{\bar{V}_n (t_{p,\text{on}} - t_1)}{(\hat{\mathbf{n}} \cdot \hat{\mathbf{k}})}, \tag{29}$$

where the values for $\bar{V}_n$ and $(\hat{\mathbf{n}} \cdot \hat{\mathbf{k}})$ can be calculated based on the topology after the $(i-1)$th pulse, or some average value may be used by iteration.

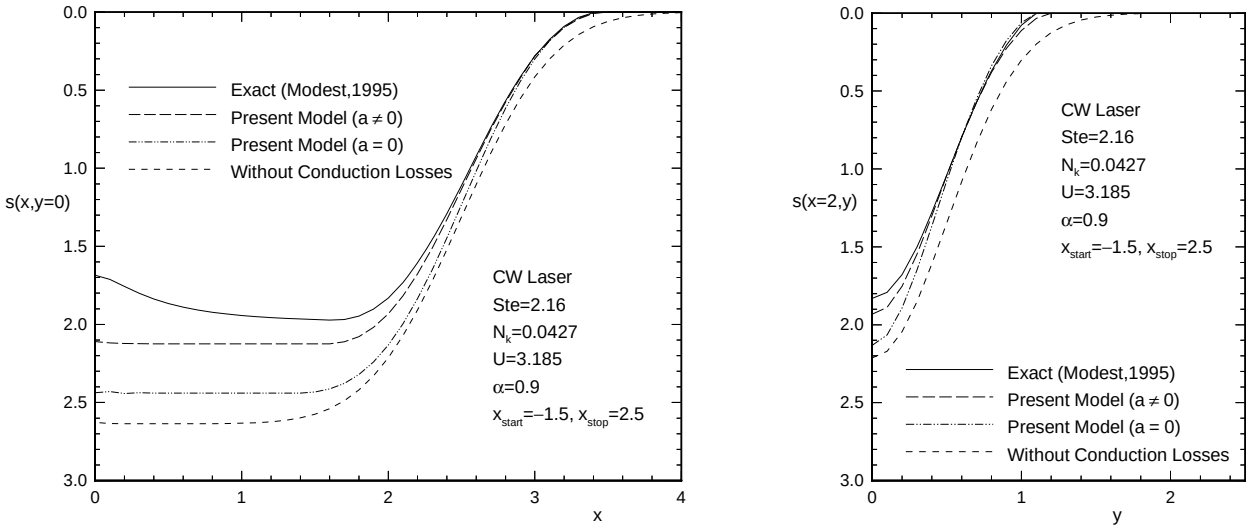

Figure 3: Groove development along centerline (left) and groove cross-section (right) for continuous-wave laser operation.

Illustrative Examples

To demonstrate the strengths and limitations of the present models, a number of example calculations are shown in Figs. 3 through 7. For simplicity, all non-dimensional parameters (except laser-on time t_p,on) were held constant at N_k = 0.0427, Ste = 2.16, U = 3.185, α = 0.9, and t_p = 0.14. This corresponds to a laser with an average power of 600 W and a radius of w_0 = 147μm scanning over graphite at 6.5 cm/s, for which a comparison with experimental data was carried out in a previous paper [Modest *et al*. (1994)]. Most laser machining operations on non-metals can be expected to have relatively similar sets of parameters. In all cases the laser is first turned on at $x_{\text{start}} = -1.5$, i.e., at a location $1.5w_0$ before the center of the laser reaches the edge of the solid, and is turned off as soon as the laser center reaches x_{stop} = 2.5.

Figure 3 shows the case of a continuous wave laser. The exact solution shows distinct entry/start-up effects, apparently due to warming up of surrounding material [Modest (1995)], which is neglected by the approximate models. At quasi-steady operation the maximum groove depth is almost $2w_0$, at which time approximately 30% of absorbed laser energy is lost to conduction (not including preheating of material, which eventually ablates). If conduction losses are neglected, a maximum depth of $2.63w_0$ is obtained (with, of course, a 30% larger overall removal rate). The

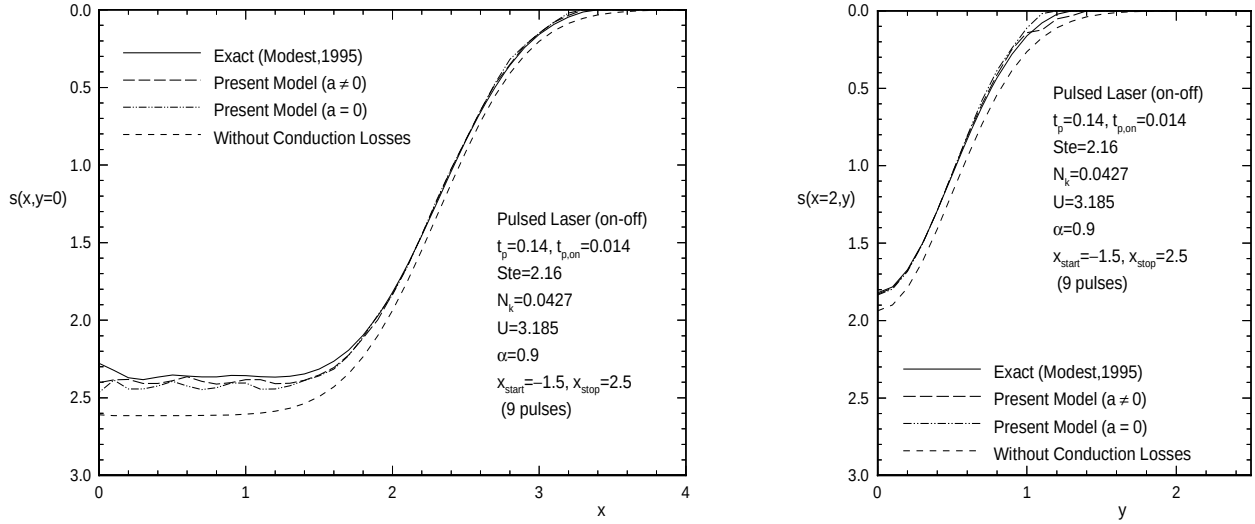

Figure 4: Groove development along centerline (left) and groove cross-section (right) for pulsed laser operation (on-off pulse shape).

approximate model does rather well if the correction factor a in equation (15) is included, predicting maximum depth to about 5% and removal rate with about 3% accuracy. For CW operation the penetration depth can be appreciable, making curvature effects important, as seen from the $a = 0$ line in the figure.

To assess whether the present integral method provides acceptable accuracy, one may apply the integral method with and without conductive losses [with and without the *transient* preheating term in equation (17); in the latter case the θ_0/δ reflects preheating of material to be ablated]. A comparison gives an estimate of the conductive losses.

Figure 4 shows the same situation for a pulsed laser with a simple on-off pulse and a 10% duty cycle ($t_{p,\mathrm{on}} = 0.1 \times t_p$, during which the laser power is ten times the average power). Conductive losses during the quasi-steady part of each laser pulse are about 10%. The curves labeled 'present model' use the full-pulse model, equation (29). While including curvature effects ($a \neq 0$) produces slightly better results, this improvement probably does not justify the considerable additional effort. Applying the full-pulse model is somewhat marginal in this case, producing groove bottom undulations much stronger than indicated by the exact solution. This is apparently due to the fact that the laser moves a distance of $U \times t_{p,\mathrm{on}}$ or $0.045 w_0$ during each laser-on time, which is neglected by the full-pulse model.

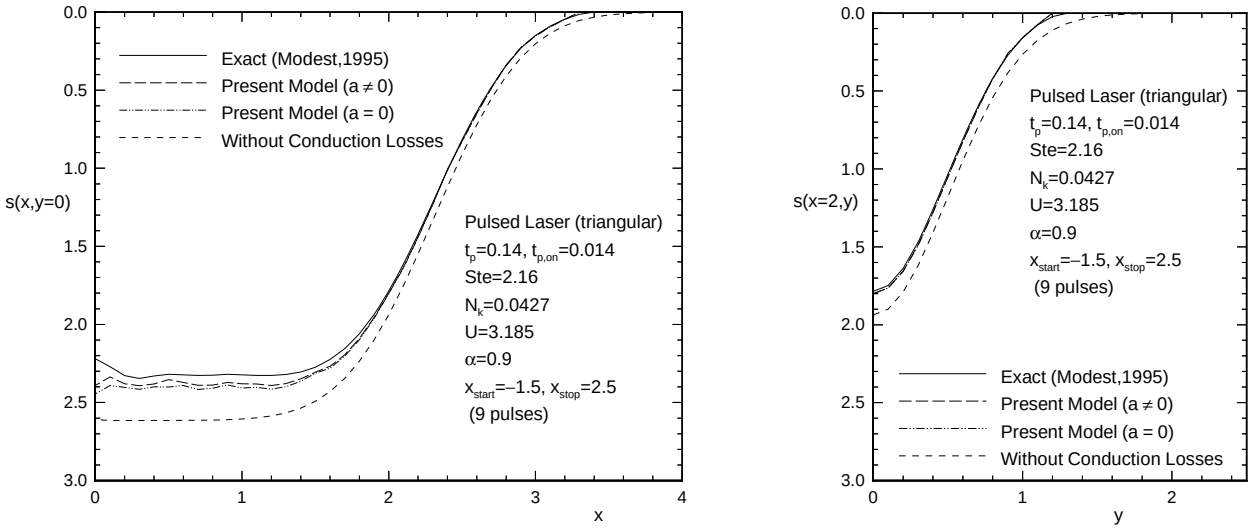

Figure 5: Groove development along centerline (left) and groove cross-section (right) for pulsed laser operation (triangular pulse shape).

The simple full-pulse model of equations (22), (24), (25), and (26) is expected to be most accurate for simple on-off pulses, for which quasi-steady ablation is reached during each pulse, equations (27) and (28). To ensure the validity of the model for arbitrary temporal pulse shapes, a triangular pulse was also considered, i.e.,

$$\phi(t) = \begin{cases} \dfrac{4t_p t}{t_{p,\,\mathrm{on}}^2}, & 0 < t < 0.5t_{p,\,\mathrm{on}}, \\ \dfrac{4t_p}{t_{p,\,\mathrm{on}}}\left(1 - \dfrac{t}{t_{p,\,\mathrm{on}}}\right), & 0.5t_{p,\,\mathrm{on}} < t < t_{p,\,\mathrm{on}}, \\ 0, & t_{p,\,\mathrm{on}} < t < t_p. \end{cases} \tag{30}$$

As Fig. 5 shows, the results are very similar. Due to the more gradual ramp-up in laser power the conduction losses are slightly larger resulting in an about 1.5% lesser groove depth. Thus, the results suggest that, for short enough pulses (10% duty cycle or less), the actual temporal variation of pulse power $\phi(t)$ is unimportant and the pulse may be replaced by a (computationally simpler) on-off pulse.

If the laser has extremely short pulses, such as a Q-switched laser, then conduction losses become negligible, regardless of pulse profile $\phi(t)$, as seen from Fig. 6 for simple on-off pulses. The "exact" solution shows a slight oscillation at the entry, which is apparently due to numerical

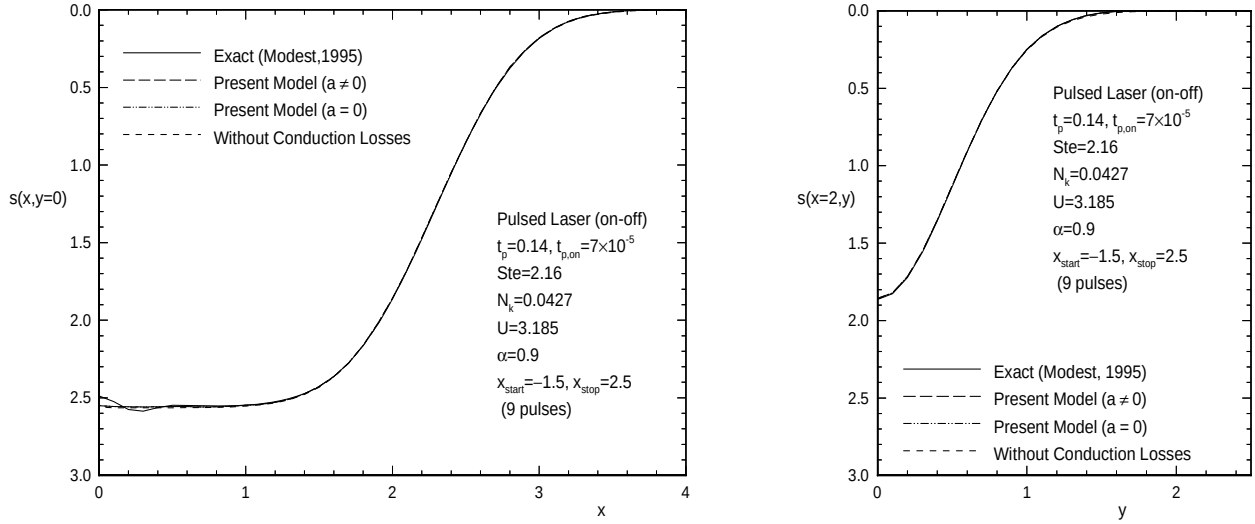

Figure 6: Groove development along centerline (left) and groove cross-section (right) for Q-switched laser operation.

instability because of the fact that at the edge interior nodes cannot be orthogonal to the top surface during transient recession. All curves virtually collapse, implying that curvature effects and, indeed, all conduction losses may be neglected, and that the full-pulse model can be applied.

Finally, Fig. 7 shows a comparison between the two approximate models for different (on-off) pulsing conditions. For small duty cycles, t_p,on$/t_p \leq 0.01$, the results from equations (17) to (20) (Integral Method) are indistinguishable from those obtained from equations (27) to (29) (Full Pulse Method). Small, but acceptable, differences become apparent for duty cycles of around 10% while the full pulse method should probably not be used for duty cycles $>$20% (or, rather, when $t_{p,\text{on}} \times U > 0.1$). In addition, for large values of $t_{p,\text{on}} \times U$ calculations with the curvature correction factor become rather unstable for $a < 0$ (as seen from the jaggedness of some of the dashed lines in Fig. 7).

Summary and Conclusions

Two simplified models have been introduced for the calculation of shapes produced by laser machining. The models are limited to opaque, strongly-absorbing materials that ablate or decompose upon irradiation by a laser (such as most ceramics), and that do not generate significant amounts of

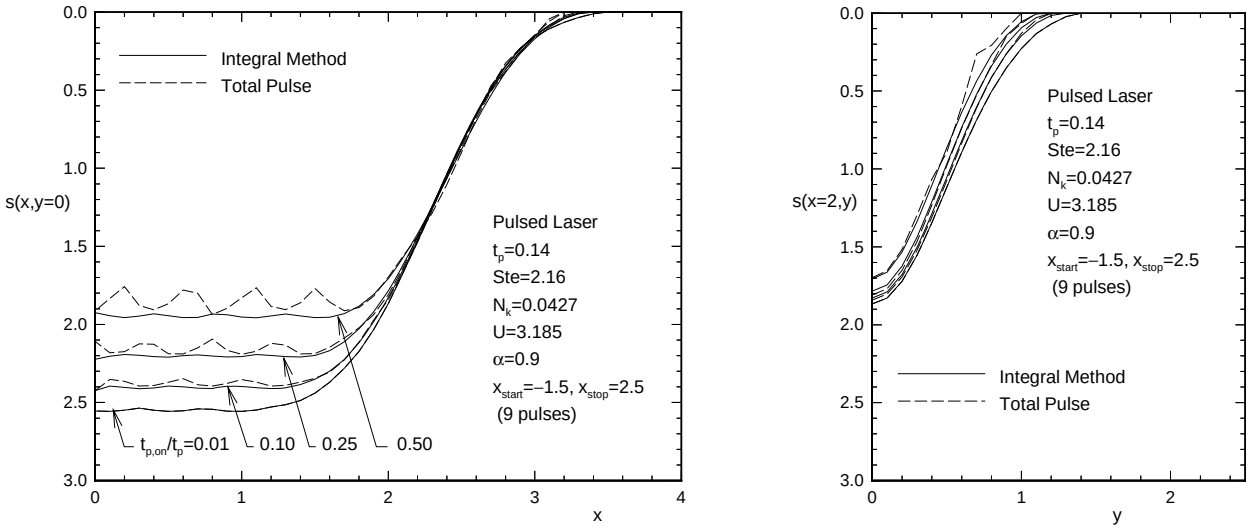

Figure 7: Groove development along centerline (left) and groove cross-section (right) for varying laser pulse lengths.

liquid in the cutting zone (as would be expected for most metals, which melt and have large thermal diffusivities). It is further assumed that any laser generated plume/plasma is blown away by strong gas-assist. The first of these models results in a time-dependent ordinary differential equation and is based on an integral method to determine conductive losses. This model is applicable to shaping with continuous-wave as well as pulsed lasers. The second model is valid only for pulsed laser operation, calculating ablation due to an entire pulse in one step. Depending on the problem at hand, spatial and temporal nodal sizes, CPU times (on a high-power workstation) are reduced from an hour or more (exact numerical) to minutes (integral method) and less than a second (full pulse method), respectively. The integral method may be applied whenever conduction losses are relatively small (less than, say, 30%). In order for the full pulse method to be valid, the laser should also not move an appreciable amount across the surface during each laser pulse (less than $\simeq 0.1\times$ laser radius).

REFERENCES

Anthony, T. R., 1980, "The Random Walk of a Drilling Laser Beam", *Journal of Applied Physics*, Vol. 51, pp. 1170–1175.

Bailey, A. W. and Modak, A., 1989, "Numerical Simulation of Laser Ablation with Cavity Reflections", *Journal of Thermophysics and Heat Transfer*, Vol. 3, No. 1, pp. 42–45.

Bang, S. Y. and Modest, M. F., 1991, "Multiple Reflection Effects on Evaporative Cutting with a Moving CW Laser", ASME JOURNAL OF HEAT TRANSFER, Vol. 113, No. 3, pp. 663–669.

Bang, S. Y. and Modest, M. F., 1992, "Evaporative Scribing with a Moving CW Laser - Effects of Multiple Reflections and Beam Polarization", In *Proceedings of ICALEO '91, Laser Materials Processing*, Vol. 74, San Jose, CA, 1992, pp. 288–304.

Bang, S. Y., Roy, S., and Modest, M. F., 1993, "CW Laser Machining of Hard Ceramics — Part II: Effects of Multiple Reflections", *International Journal of Heat and Mass Transfer*, Vol. 36, No. 14, pp. 3529–3540.

Bunting, K. A. and Cornfield, G., February 1975, "Toward a General Theory of Cutting: A Relationship Between the Incident Power Density and the Cut Speed", ASME JOURNAL OF HEAT TRANSFER, pp. 116–121.

Chryssolouris, G., 1991, *Laser Machining: Theory and Practice*, Springer Verlag, New York, NY, 1st ed.

Dabby, F. W. and Paek, U.-C., 1972, "High-Intensity Laser-Induced Vaporization and Explosion of Solid Material", *IEEE Journal of Quantum Electronics*, Vol. QE-8, pp. 106–111.

Kogelnik, H. and Li, T., 1956, "Laser Beams and Resonators", *Applied Optics*, Vol. 5, No. 10, pp. 1550–1565.

Luxon, J.T. and Parker, D.E., 1985, *Industrial Lasers and Their Applications*, Prentice-Hall, Englewood Cliffs, NJ, 1st ed.

Modest, M. F. and Abakians, H., 1986, "Evaporative Cutting of a Semi-Infinite Body With a Moving CW Laser", ASME JOURNAL OF HEAT TRANSFER, Vol. 108, pp. 602–607.

Modest, M. F., Ramanathan, S., Raiber, A., and Angstenberger, B., 1994, "Laser Machining of Ablating Materials–Overlapped Grooves and Entrance/Exit Effects", In *Proceedings of ICALEO '94*, to appear in *Journal of Laser Applications*.

Modest, M. F., 1995, "Three-Dimensional, Transient Model for Laser Machining of Ablating Materials", *International Journal of Heat and Mass Transfer*, in print.

Petring, D., Abels, P., and Beyer, E., 1988, "Absorption Distribution on Idealized Cutting Front Geometries and Its Significance for Laser Beam Cutting", In *High Power CO_2 Laser Systems*

and Applications, Bellingham, Washington, 1988, SPIE, pp. 123–131.

Ramanathan, S. and Modest, M. F., 1990, "Effect of Variable Properties on Evaporative Cutting with a Moving CW Laser", In *Heat Transfer in Space Systems*, Vol. HTD–135, ASME, pp. 101–108.

Ramanathan, S. and Modest, M. F., 1992a, "CW Laser Cutting of Composite Ceramics", In *Laser Advanced Materials Processing – LAMP '92*, Vol. 2, Nagaoka, Japan, 1992, pp. 625–632.

Ramanathan, S. and Modest, M. F., 1992b, "CW Laser Drilling of Composite Ceramics", In *Proceedings of ICALEO '91, Laser Materials Processing*, Vol. 74, San Jose, CA, 1992, pp. 305–326.

Ramanathan, S. and Modest, M. F., 1993, "Measurement of Temperatures and Absorptances for Laser Processing Applications", In *ICALEO '93*, Orlando, FL, 1993.

Ramanathan, S. and Modest, M. F., 1995, "High-Speed Photographic Visualization of Laser Processing Phenomena", *Journal of Laser Application*, Vol. 7, pp. 75–82.

Roy, S. and Modest, M. F., 1993, "Evaporative Cutting with a Moving CW Laser — Part I: Effects of Three-Dimensional Conduction and Variable Properties", *International Journal of Heat and Mass Transfer*, Vol. 36, No. 14, pp. 3515–3528.

Schuöcker, D. and Müller, P., 1987, "Dynamic Effects in Laser Cutting and Formation of Periodic Striations", In *Proceedings of the SPIE*, Vol. 801, pp. 258–264.

von Allmen, M., 1976, "Laser Drilling Velocity in Metals", *Journal of Applied Physics*, Vol. 47, pp. 5460–5463.

Vorreiter, J. O., Kaminski, D. A., and Smith, R. N., 1991, "MonteCarlo Simulation of a Laser Drilling Process", ASME paper no. 91-WA-HT-9.

Wagner, R. E., 1974, "Laser Drilling Mechanics", *Journal of Applied Physics*, Vol. 45, pp. 4631–4637.